Inorg. Chem. **2008**, *47*, 10017−10024

Racemic Atropisomeric N,N-Chelate Ligands for Recognizing Chiral Carboxylates via Zn(II) Coordination: Structure, Fluorescence, and Circular Dichroism

Theresa M. McCormick and Suning Wang*

Department of Chemistry, Queen's University, Kingston, Ontario K7L 3N6, Canada

Received July 7, 2008

Two racemic atropisomeric N,N′-chelate ligands, bis{3,3′-[*N*-Ph-2-(2′-py)indolyl]} (**1**) and bis{3,3′-*N*-4-[*N*-2-(2′-py)indolyl]phenyl-2-(2′-py)indolyl} (**2**), have been found to be able to distinguish the enantiomers of Zn((*R*)-BrMeBu)$_2$ and Zn((*S*)-BrMeBu)$_2$ where BrMeBu = $O_2CCH(Br)CHMe_2$, with a distinct and intense CD spectral response at approximately the 10 μM concentration range. Computational studies established that the (*R*)-**1**-Zn((*R*)-BrMeBu)$_2$ or (*S*)-**1**-Zn((*S*)-BrMeBu)$_2$ diastereomer is more stable than (*R*)-**1**-Zn((*S*)-BrMeBu)$_2$ or (*S*)-**1**-Zn((*R*)-BrMeBu)$_2$. In addition, computational studies showed that the CD spectra of (*S*)-**1**-Zn((*S*)-BrMeBu)$_2$ and (*S*)-**1**-Zn((*R*)-BrMeBu)$_2$ are similar. ^{1}H NMR spectra confirmed that these two diastereomers exist in solution in about a 2:1 ratio for both complexes of **1** and **2**. The distinct CD response of the racemic ligands **1** and **2** toward the chiral zinc(II) carboxylate is therefore attributed to the preferential formation of one diastereomer. The binding modes of the zinc(II) salt with ligands **1** and **2** were established by the crystal structures of the model compounds **1**-Zn(tfa)$_2$ and **2**-Zn(tfa)$_2$ (tfa = $CF_3CO_2^-$), where the Zn^{II} ion is chelated by the two central pyridyl groups in the ligand. Fluorescent titration experiments with various zinc(II) salts showed that the fluorescent spectrum of the atropisomeric ligand displays an anion-dependent change. The zinc(II) binding strength to the N,N′-chelate site of the atropisomeric ligand has been found to play a key role in the selective recognition of different chiral zinc(II) carboxylate derivatives by the racemic atropisomeric ligands.

Introduction

Chiral sensing is an important and intensive research field because of its broad applications in probing and understanding chiral recognition events in biological systems, the development of chiral catalytic systems, and the syntheses of new chiral drugs.[1] Among the various physical methods for fast and sensitive chiral sensing and the determination of enantiomeric excess (ee), circular dichroism (CD) is the most commonly used one. In order for CD to work effectively, however, either the chiral host or the chiral guest must have strong absorption in the UV−vis region and the resulting host−guest complexes must have distinct CD spectra.[2] Many examples of using enantiomerically pure host molecules for chiral sensing by CD detection methods are known in the literature.[3] Supramolecular hosts that produce a CD signal when interacting with a chiral guest have been shown to be viable chiral sensors.[4] Many achiral supramolecular hosts such as porphyrin derivatives have been shown

* To whom correspondence should be addressed. E-mail: Wangs@chem.queensu.ca.

(1) (a) Gottarelli, G.; Lena, S.; Masiero, S.; Pieraccini, S.; Spada, G. P. *Chirality* **2008**, *20*, 471. (b) Mateos-Timoneda, M. A.; Crego-Calama, M.; Reinhoudt, D. N. *Chem. Soc. Rev.* **2004**, *33*, 363. (c) Matsushita, H.; Yamamoto, N.; Meijler, M. M.; Whirching, P.; Lerner, R. A.; Matsushita, M.; Janda, K. D. *Mol. BioSyst.* **2005**, *1*, 303. (d) Takeuchi, M.; Mizuno, T.; Shinkai, S.; Shirakami, S.; Itoh, T. *Tetrahedron: Asymmetry* **2000**, *11*, 3311. (e) Lee, S. J.; Lin, W. B. *J. Am. Chem. Soc.* **2002**, *124*, 4554. (f) Ma, L.; White, P. S.; Lin, W. B. *J. Org. Chem.* **2002**, *67*, 7577. (g) Tan, H. Q.; Li, Y. G.; Zhang, Z. M.; Qin, C.; Wang, X. L.; Wang, E. B.; Su, Z. M. *J. Am. Chem. Soc.* **2007**, *129*, 10066. (h) Dybtsev, N. N.; Nuzhdin, A. L.; Chun, H.; Bryliakov, K. P.; Talsi, E. P.; Fedin, V. P.; Kim, K. *Angew. Chem., Int. Ed.* **2006**, *45*, 916.

(2) (a) Fischbeck, A.; Bartke, N.; Humpf, H. U. *Monatsh. Chem.* **2005**, *136*, 397, and references cited therein. (b) Hayashi, T.; Aya, T.; Nonoguchi, M.; Mitzutani, T.; Hiseda, Y.; Kitagawa, S.; Ogoshi, H. *Tetrahedron* **2002**, *58*, 2803.

(3) (a) Maeda, K.; Morioka, K.; Yashima, E. *Macromolecules* **2007**, *40*, 1349. (b) Kim, W.; So, S. M.; Chagal, L.; Lough, A. J.; Kim, B. M.; Chin, J. *J. Org. Chem.* **2006**, *71*, 8966. (c) Li, Z.-B.; Pu, L. *J. Mater. Chem.* **2005**, *15*, 2860. (d) Lin, J.; Rajaram, A. R.; Pu, L. *Tetrahedron* **2004**, 11277. (e) Chen, Z.-H.; He, Y.-B.; Hu, C.-G.; Huang, X.-H.; Hu, L. *Aust. J. Chem.* **2008**, *61*, 310. (f) Pu, L. *Chem. Rev.* **2004**, *104*, 1687. (g) Nieto, S.; Lynch, V. M.; Anslyn, E. V.; Kim, H.; Chin, J. *J. Am. Chem. Soc.* **2008**, *130*, 9232.

10.1021/ic801269z CCC: $40.75
Published on Web 10/03/2008

Chart 1

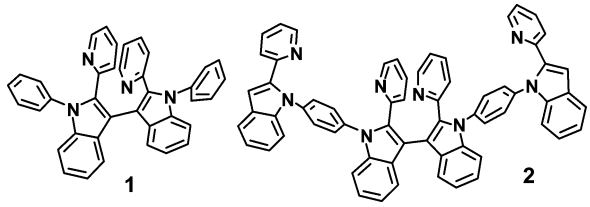

to be able to act as chiral sensors via induced chirality upon binding with chiral guest molecules.[5] Certain racemates and biological molecules such as DNA have been demonstrated to be effective in chiral sensing using CD methods.[6] Examples of chiral sensing of organic molecules mediated by metal−ligand interactions, albeit relatively uncommon, are also known in the literature.[7] Recently, we reported a new class of N,N-chelate atropisomeric ligands including **1** and **2** shown in Chart 1. Although we have not been able to resolve the enantiomers of **1** and **2**, we have shown that the racemate **1** can bind to a Cu^{I} ion to form racemic homochiral complexes that upon resolution by hand-picking of the crystals display distinct CD spectra.[8] Further investigation on this system has led to the discovery that the racemic atropisomers **1** and **2** can be used directly for sensing certain chiral zinc(II) carboxylates such as (*S*)-2-bromo-3-methylbutyrate ((*S*)-BrMeBu) and (*R*)-2-bromo-3-methylbutyrate ((*R*)-BrMeBu) and determining the ee by CD methods. The zinc(II) binding to the chelates **1** and **2** is inevitably affected by the carboxylate binding ability to the zinc(II) center, which has been found to play a key role in the CD response. The details of our investigation are reported herein.

Experimental Section

All starting materials were purchased from Aldrich Chemical Co. and used without further purification. Solvents were freshly distilled over appropriate drying reagents under a N_2 atmosphere. Thin-layer chromatography was carried out on silica gel. Flash chromatography was carried out on silica (silica gel 60, 70−230 mesh). All UV−vis spectra were collected by using an Ocean Optics Inc. spectrometer and Spectra Suite software. ^{1}H NMR spectra were recorded on a Bruker Avance 500 MHz spectrometer. Excitation and emission spectra were recorded on a Photon Technologies International QuantaMaster model C-60 spectrometer. The CD spectra were recorded on a Jasco 715 CD spectrometer with a 1 cm path length. Elemental analyses were performed by Canadian Microanalytical Service Ltd., Delta, British Columbia, Canada, or at the University of Toronto, Toronto, Ontario, Canada. Ligands **1** and **2** were prepared using our recently reported procedures.[8]

Synthesis of Zn(BrMeBu)$_2$. A total of 1 mmol of ZnO and 2 mmol of (*R*)- or (*S*)-2-bromo-3-methylbutyric acid were added to 10 mL of degassed toluene. The mixture was stirred under N_2 overnight, and the solvent was removed under vacuum. The residue was dissolved in tetrahydrofuran (THF). After removal of the insoluble solid, the solvent was evaporated to give the product. The racemic salt can be made in the same manner by using racemic 2-bromo-3-methylbutyric acid.

Synthesis of 1-Zn(tfa)$_2$. A solution of 82 mg (0.280 mmol) of Zn(tfa)$_2$ in ∼5 mL of THF was layered on top of a solution of 150 mg (0.280 mmol) of **1** in ∼5 mL of CH_2Cl_2. Slow diffusion of the layers resulted in light-yellow crystals of the complex in 44% yield in ca. 5 days. ^{1}H NMR in CD_2Cl_2 (δ, ppm, 223 K): 6.97−7.00 (m, 3H), 7.22−7.25 (m, 1H), 7.29 (dd, J = 7.5 and 7.5 Hz, 1H), 7.36 (d, J = 5.0 Hz, 1H), 7.39−7.41 (m, 2H), 7.47 (dd, J = 7.5 and 7.5 Hz, 1H), 7.70 (dd, J = 7.5 and 7.5 Hz, 1H), 7.87 (dd, J = 7.5 and 7.5 Hz, 1H), 7.92 (d, J = 5.0 Hz, 1H), 8.68 (d, J = 5.0 Hz, 1H). Anal. Calcd for $C_{42}H_{26}F_6N_4O_4Zn$: C, 60.77; H, 3.15; N, 6.75. Found: C, 60.65; H, 3.16; N, 6.60.

Synthesis of 2-Zn(tfa)$_2$. A solution 75 mg (0.081mmol) of **2** in ∼10 mL of CH_2Cl_2 was layered with a solution of 24 mg (0.081 mmol) of Zn(tfa)$_2$ in THF. The layers were allowed to slowly mix. As the solvents evaporated, a yellow powder precipitated. The solution was decanted, and the powder was recrystallized from CH_2Cl_2 and hexanes to afford light-yellow crystals (∼50%). ^{1}H NMR in CD_2Cl_2 (500 MHz, δ, ppm, 298 K): 8.76 (d, J = 5 Hz, 1H), 8.48 (d, J = 5 Hz, 1H), 7.95 (dd, J = 7.5 and 7.5 Hz, 1H), 7.78 (d, J = 5 Hz, 1H), 7.69 (dd, J = 7.5 and 7.5 Hz, 1H), 7.62 (br s, 2H), 7.51−7.44 (m, 6H), 7.38 (d, J = 10 Hz, 1H), 7.34−7.30 (m, 2H), 7.26 (dd, J = 7.5 and 7.5 Hz, 1H), 7.21 (dd, J = 5 and 5 Hz, 1H), 7.17 (s, 1H), 7.04 (s, 2H). Anal. Calcd for $C_{68}H_{42}F_6N_4O_4Zn\cdot 3.5CH_2Cl_2$: C, 56.81; H, 3.27; N, 7.41. Found: C, 56.43; H, 3.14; N, 7.59.

Syntheses of 1-Zn((*S*)-BrMeBu)$_2$ and 2-Zn((*S*)-BrMeBu)$_2$. These two compounds were synthesized on an NMR scale, by combining 4.7 mg (8.8 μmol) of **1** with 3.8 mg (9.1 μmol) of Zn((*S*)-BrMeBu)$_2$ or 5.8 mg (6.3 μmol) of **2** with 2.8 mg (6.5 μmol) of Zn((*S*)-BrMeBu)$_2$ in the same manner as that for the Zn(tfa)$_2$ complexes. Both compounds were characterized by ^{1}H NMR spectra. ^{1}H NMR for **1**-Zn((*S*)-BrMrBu)$_2$ in CD_2Cl_2 (500 MHz, δ, ppm, 203 K): 8.73 (d, J = 5 Hz, 0.35H, *o*-H, py, minor diastereomer), 8.70 (d J = 5 Hz, 0.65H, *o*-H, py, major diastereomer), 7.88 (d, J = 10 Hz, 1H), 7.77 (dd, J = 7.5 and 7.5 Hz, 1H), 7.67 (dd, J = 7.5 and 7.5 Hz 1H), 7.45−7.41 (m, 3H), 7.37 (dd, J = 7.5 and 7.5 Hz, 1H), 7.34−7.31 (m, 2H), 7.27−7.18 (m, 2H), 6.97 (d, J = 5 Hz, 1H), 6.92 (d, J = 10 Hz, 1H), 4.12 (d, J = 5 Hz, 0.65H, α-H, BrMeBu, major diasteromer), 3.91 (d, J = 5 Hz, 0.35H, α-H, BrMeBu, minor diastereomer), 1.93 (m, 1H), 0.61 (s, 6H). ^{1}H NMR **2**-Zn((*S*)-BrMrBu)$_2$ in CD_2Cl_2 (500 MHz, δ, ppm, 298 K): 8.86 (d, J = 5 Hz, 1 H), 8.52 (s, 1H), 7.88−7.77 (m, 3H), 7.68 (dd, J = 7.5 and 7.5 Hz, 1H), 7.51 (d, J = 10 Hz, 1H),

(4) (a) Hembury, G. A.; Borovkov, V. V.; Inoue, Y. *Chem. Rev.* **2008**, *108*, 1. (b) Bhyrappa, P.; Borokov, V. V.; Inoue, Y. *Org. Lett.* **2007**, *9*, 433. (c) Ikeda, H.; Li, Q.; Ueno, A. *Bioorg. Med. Chem. Lett.* **2006**, *16*, 5420. (d) Mateos-Timoneda, M. A.; Crego-Calama, M.; Reinhoudt, D. N. *Chem. Soc Rev.* **2004**, *33*, 363. (e) Ishi-I, T.; Crego-Calama, M.; Timmerman, P.; Reinhoudt, D. N.; Shinkai, S. *Angew. Chem., Int. Ed.* **2002**, *41*, 1924. (f) Huang, X.; Nakanishi, K.; Berova, N. *Chirality* **2000**, *12*, 237. (g) Piguet, C.; Bernardinelli, G.; Hopfgartner, G. *Chem. Rev.* **1997**, *97*, 2005.

(5) (a) Li, W.-S.; Jiang, D.-L.; Suna, Y.; Aida, T. *J. Am. Chem. Soc.* **2005**, *127*, 7700. (b) Allenmark, S. *Chirality* **2003**, *15*, 409. (c) Proni, G.; Pescitelli, G.; Huang, X.; Quraishi, N. Q.; Nakanishi, K.; Berova, N. *Chem. Commun.* **2002**, 1590. (d) Kurtan, T.; Nasri, N.; Li, Y.-Q.; Hang, X.; Nakanishi, K.; Berova, N. *J. Am. Chem. Soc.* **2001**, *123*, 5962.

(6) (a) Maeda, K.; Yahima, E. *Top. Curr. Chem.* **2006**, *265*, 47. (b) Krois, D.; Lehner, H. *J. Chem. Soc., Perkin Trans. 2* **1995**, 489. (c) Barton, J. K.; Dannenberg, J. J.; Raphael, A. L. *J. Am. Chem. Soc.* **1982**, *104*, 4967. (d) Barton, J. K.; Lolis, E. *J. Am. Chem. Soc.* **1985**, *107*, 708. (e) Önfelt, B.; Lincoln, P.; Norden, B. *J. Am. Chem. Soc.* **2001**, *123*, 3630.

(7) (a) Gao, F.; Ruan, W.-J.; Chen, J.-M.; Zhang, Y.-H.; Zhu, Z.-A. *Spectrochem. Acta, Part A* **2005**, *62*, 886. (b) Anderberg, P. I.; Turner, J. J.; Evans, K. J.; Hutchins, L. M.; Harding, M. M. *Dalton Trans.* **2004**, 1708. (c) Tsukube, H.; Shinoda, S.; Tamiaki, H. *Coord. Chem. Rev.* **2002**, 227. (d) Tsukube, H.; Hosokubo, M.; Wada, M.; Shinoda, S.; Tamiaki, H. *Inorg. Chem.* **2001**, *40*, 740. (e) Meskers, S. C. J.; Dekkers, H. P. J. M. *J. Phys. Chem. A* **2001**, *105*, 4589. (f) Kurtán, T.; Nesnas, N.; Li, Y.-Q.; Huang, X.; Nakanishi, K.; Berova, N. *J. Am. Chem. Soc.* **2001**, *123*, 5962. (g) Dai, L.-X.; Zhou, Z.-H.; Zhang, Y.-Z.; Zhou, Y.-F. *J. Chem. Soc., Chem. Commun.* **1987**, 1760.

(8) McCormick, T. M.; Liu, Q.; Wang, S. *Org. Lett.* **2007**, *9*, 4087.

Table 1. Selected Bond Lengths (Å) and Angles (deg)

Compound **1**-Zn(tfa)$_2$			
Zn(1)−O(1)	1.9890(13)	O(4)−Zn(1)−O(1)	106.11(6)
Zn1(1)−O(4)	1.9872(14)	O(4)−Zn(1)−N(1)	102.53(6)
Zn(1)−N(1)	2.0557(15)	O(1)−Zn(1)−N(1)	95.57(6)
Zn(1)−N(4)	2.0655(15)	O(4)−Zn(1)−N(4)	105.34(6)
		O(1)−Zn(1)−N(4)	105.34(6)
		N(1)−Zn(1)−N(4)	140.81(6)
Compound **2**-Zn(tfa)$_2$			
Zn(1)−O(2)	1.9716(17)	O(2)−Zn(1)−O(2′)	119.57(11)
Zn1(1)−N(1)	2.061(2)	O(2)−Zn(1)−N(1)	102.60(7)
		O(2)−Zn(1)−N(1′)	98.20(7)
		N(1)−Zn(1)−N(1′)	137.99(11)

7.46−7.39 (m, 6H), 7.33−7.24 (m, 4H), 7.21 (dd, J = 5 and 5 Hz, 1H), 7.18 (s, 1H), 7.05 (d, J = 10 Hz, 1H), 7.01 (dd, J = 5 and 5 Hz, 1H), 3.99 (s, 1H), 1.71 (m, 1H), 0.32 (s, 6H).

Molecular Orbital Calculations. The ground-state molecular geometry optimizations were performed for (*S*)-**1**-Zn((*R*)-BrMeBu)$_2$ and (*S*)-**1**-Zn((*S*)-BrMeBu)$_2$. The geometric parameters from X-ray diffraction analysis of **1**-Zn(tfa)$_2$ were modified and used as the starting point for the geometry optimization. The Gaussian suite of programs (*Gaussian 03*)[9] was used with the B3LYP/6-311G(d) basis set employing a restricted Hartree−Fock level of computation. CD spectra for both diastereomers were computed by time-dependent density functional theory (TD-DFT) calculations using the optimized geometrical parameters and the same basis set. The first 25 singlet states were calculated.

Titration Experiments. For typical CD and fluorescent titration experiments, a 1×10^{-5} M solution of **1** or **2** in CH_2Cl_2 was prepared. A total of 0.1 mol equiv of a 1×10^{-2} M solution of zinc(II) salt in THF was added with a micropipette and mixed for 2 min before recording of the spectrum. The NMR titration experiment was carried out with ∼5 mg of **1** or **2** in CD_2Cl_2 in an NMR tube, and a 1.0 M solution of Zn((*R*)- BrMeBu)$_2$ in CD_3OD was added incrementally with a micropipette.

X-ray Crystallographic Analysis. Single crystals of **1**-Zn(tfa)$_2$ and **2**-Zn(tfa)$_2$ were mounted on glass fibers for data collection. Data were collected at ambient temperature for **1**-Zn(tfa)$_2$ at 180 K for **2**-Zn(tfa)$_2$ on a Bruker Apex II single-crystal X-ray diffractometer with graphite-monochromated Mo Kα radiation, operating at 50 kV and 30 mA. The crystals of **1**-Zn(tfa)$_2$ belong to the triclinic space group $P\bar{1}$, while the crystals of **2**-Zn(tfa)$_2$ belong to the monoclinic space group $C2/c$. No significant decay was observed for both samples. Data were processed on a PC using the Bruker *SHELXTL* software package (version 5.10) and are corrected for absorption effects. The structures were solved by direct methods. One of the CF_3 groups in **1**-Zn(tfa)$_2$ displays rotational disordering, which was modeled and refined successfully. All non-H atoms were refined anisotropically. Selected bond lengths and angles are provided in Table 1. Complete crystal data can be found in the Supporting Information.

Results and Discussion

Binding Modes and Structures of Complexes of Zinc(II) Carboxylates with Ligands 1 and 2. The chiral recognition study focused on two chiral zinc(II) carboxylates: (*S*)-BrMeBu and (*R*)-BrMeBu. To establish the binding mode of the chiral zinc(II) carboxylate with the chelate ligands **1** and **2**, we attempted to obtain single crystals of the complexes for X-ray diffraction analysis. However, no crystals suitable for X-ray diffraction were obtained for the complexes of Zn(BrMeBu)$_2$. We therefore focused our efforts on obtaining single crystals of the nonchiral zinc(II) carboxylate, Zn(tfa)$_2$, tfa = $CF_3CO_2^-$ with ligands **1** and **2**. Fortunately, single crystals of both complexes **1**-Zn(tfa)$_2$ and **2**-Zn(tfa)$_2$ were obtained, and their structures were successfully determined by X-ray diffraction. Both complexes were found to be 1:1 adducts of the ligand with Zn(tfa)$_2$.

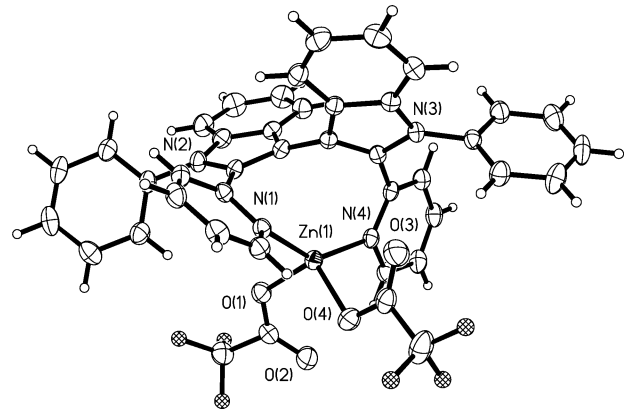

Figure 1. Structure of **1**-Zn(tfa)$_2$ with 50% thermal ellipsoids and labeling schemes for the key atoms. Only one set of disordered F atoms are shown for clarity.

Structures of 1-Zn(tfa)$_2$ and 2-Zn(tfa)$_2$. As shown in Figure 1, the molecule of **1**-Zn(tfa)$_2$ has an approximate C_2 symmetry, with the Zn center being chelated by two pyridyl groups of ligand **1**. The dihedral angle between the two indolyl rings is 118.1°, which is considerably smaller than that of the free ligand (125.1°),[8] indicating a greater twist between the two rings due to zinc(II) coordination. The two tfa anions are bound to the Zn center as terminal ligands. The Zn−N [2.056(1)−2.065(1) Å] and Zn−O [1.987(1)−1.989 (1) Å] bond lengths are normal;[1g,h,10,11] however, the geometry around the Zn^{II} ion is a highly distorted tetrahedron with a very large N−Zn−N angle, 140.81(6)°, resembling that observed in the structure of $[Cu(\mathbf{1})_2]^+$.[8] Consistent with the behavior of the copper(I) complex reported earlier, the phenyl group on ligand **1** in **1**-Zn(tfa)$_2$ displays a hindered rotation around the C−N bond in solution due to nonbonding hydrogen interactions between the phenyl, the indolyl, and the pyridyl groups, as confirmed by variable-temperature ^{1}H NMR spectra of **1**-Zn(tfa)$_2$ (see the Supporting Information).

The crystals of **2**-Zn(tfa)$_2$ are very small and not very uniform. Fortunately, some of the crystals produced sufficient diffractions when used in X-ray diffraction experiments, hence allowing the determination of the structure of **2**-Zn(tfa)$_2$ shown in Figure 2. The molecule of **2**-Zn(tfa)$_2$ has a

(9) Frisch,M. J.; et al. *Gaussian 03*, revision C.02; Gaussian, Inc.: Wallingford, CT, 2004.

(10) Wu, Q.; Lavigne, J. A.; Tao, Y.; D'Iorio, M.; Wang, S. *Inorg. Chem.* **2000**, *39*, 5248.

(11) (a) Liu, S.-F.; Wu, Q.; Schmider, H. L.; Aziz, H.; Hu, N.-X.; Popovic, Z.; Wang, S. *J. Am. Chem. Soc.* **2000**, *122*, 3671. (b) Prince, R. H. In *Comprehensive Coordination Chemistry*; Wilkinson, G., Gillard, R. D., McCleverty, J. A., ed.; Pergamon Press: New York, 1987; Vol. *5*, Chapter 56.1. (c) Kerr, M. C.; Preston, H. S.; Ammon, H. L.; Huheey, J. E.; Stewart, J. M. *J. Coord. Chem.* **1981**, *11*, 111. (d) Pang, J.; Marcotte, E. J.-P.; Seward, C.; Brown, R. S.; Wang, S. *Angew. Chem., Int. Ed.* **2001**, *40*, 4042.

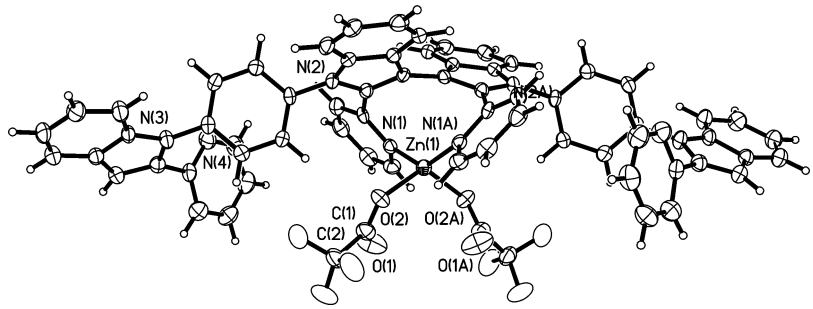

Figure 2. Structure of **2**-Zn(tfa)$_2$ with 50% thermal ellipsoids and labeling schemes for the key atoms.

Chart 2

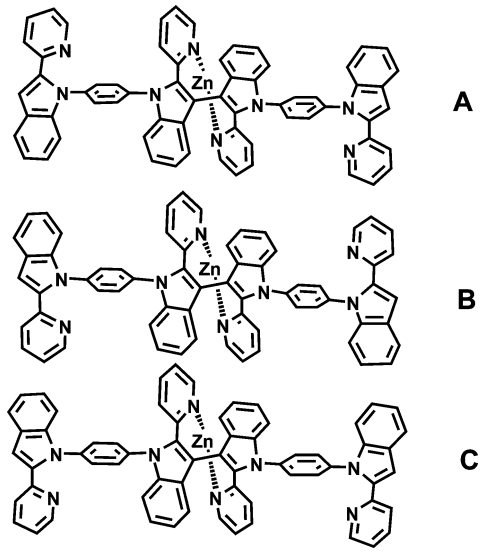

crystallographically imposed C_2 symmetry. The Zn^{II} ion is bound to the two central pyridyl rings of ligand **2** in the same manner as that in **1**-Zn(tfa)$_2$ with similar Zn−O and Zn−N bond lengths. One notable difference is the bond angles of O−Zn−O [106.11(6)° for **1**-Zn(tfa)$_2$ and 119.57(11)° for **2**-Zn(tfa)$_2$] and N−Zn−N [140.81(6)° for **1**-Zn(tfa)$_2$ and 139.99(11)° for **2**-Zn(tfa)$_2$]. The much smaller O−Zn−O bond angle in **1**-Zn(tfa)$_2$ is likely caused by the relatively short separation distance between the noncoordinating O(3) atom and the Zn^{II} ion [2.836(1) Å], which is much shorter than that between O(2) and Zn(1) [3.003(1) Å] in **2**-Zn(tfa)$_2$ [106.11(6)°]. The dihedral angle between the two central indolyl rings in **2**-Zn(tfa)$_2$ is 128.8°, much greater than that in **1**-Zn(tfa)$_2$ but nearly identical with that of the free ligand **2** (128.5°). The inner indolyl ring and the outer indolyl ring are not coplanar with the phenyl linker with dihedral angles of 122.7° and 126.1°, respectively, with respect to the phenyl plane, which is again caused by nonbonding interactions of H atoms between the 2-(2-py)indolyl group and the phenyl. Significantly, in the crystal structure of **2**-Zn(tfa)$_2$, the two neighboring inner and outer 2-(2-py)indolyl groups are on the same side with respect to the phenyl plane, i.e., having syn−syn geometry, **A**, shown in Chart 2. The coordination of the two central py rings to the Zn^{II} ion forces the two central 2-(2-py)indolyls to orient in opposite directions (dihedral angle, 128.8°). As a result, the other possible geometric isomers are anti−anti and syn−anti, shown as **B** and **C**, respectively, in Chart 2. Variable-temperature ^{1}H NMR data of **2**-Zn(tfa)$_2$ appear to indicate that there are two dominating isomers in solution with about a 1:1 ratio (see the Supporting Information), based on the appearance of two distinct H_1−py chemical shifts at low temperature. However, it is possible that the chemical shifts of isomer **C** overlap with those of **A** and **B**, making it difficult to determine the precise distributions of the three isomers in solution. Nonetheless, the structural isomerism observed in **2**-Zn(tfa)$_2$ is not surprising because of their similarity with that observed in platinum(II) and copper(I) complexes based on 1,3- and 1,4-bis[2-(2-py)benzimidazolyl]benzene ligands.[12]

Structures of 1-Zn((*S*)-BrMeBu)$_2$ and 2-Zn((*S*)-BrMeBu)$_2$ in Solution. The chiral zinc(II) salt Zn((*S*)-BrMeBu)$_2$ or Zn((*R*)-BrMeBu)$_2$ was found to bind to ligands **1** and **2** in the same manner as Zn(tfa)$_2$, based on the similarity of the ^{1}H NMR data of **1**-Zn((*S*)-BrMeBu)$_2$ and **2**-Zn((*S*)-BrMeBu)$_2$ with those of **1**-Zn(tfa)$_2$ and **2**-Zn(tfa)$_2$. However, the presence of the chiral center on the BrMeBu ligand can lead to the formation of diastereomers. For example, diastereomers (*R*)-**1**-Zn((*S*)-BrMeBu)$_2$ and (*S*)-**1**-Zn((*S*)-BrMeBu)$_2$ are expected when Zn((*S*)-BrMeBu)$_2$ is reacted with the racemate **1**. ^{1}H NMR titration experiments indeed show that when less than 1 equiv of Zn((*S*)-BrMeBu)$_2$ is added to the solution of **1** in CD_2Cl_2, two sets of well-resolved chemical shifts for both H_1-py and H_α-BrMeBu protons with a ∼2:1 ratio are observed (see Figure 3 and the Supporting Information), which can be attributed to the two diastereomers. ^{1}H NMR titration experiments also confirmed that Zn(BrMeBu)$_2$ binds to **1** fairly strongly because of the fact that the free ligand and the bound ligand have distinct and well-resolved signals when the Zn^{II}:**1** ratio is less than 1 (Figure 3). When more than 1 equiv of Zn((*R*)-BrMeBu)$_2$ is added, the diastereomer peaks are no longer resolved at ambient temperature, which can be attributed to the dynamic exchange between bound and nonbound Zn((*R*)-BrMeBu)$_2$. For the 1:1 complex **1**-Zn((*R*)-BrMeBu)$_2$, the diastereomer peaks can be resolved at ∼203 K with the same 2:1 integrated intensity ratio as was observed in the NMR titration experiments (see the Supporting Information). The variable-temperature ^{1}H NMR spectra of **2**-Zn((*R*)-BrMeBu)$_2$ is complex because of the presence of geometric isomers and diastereoisomers associated with each geometric isomer. Similar geometric isomeric peaks are observed in **2**-Zn((*R*)-

(12) (a) Liu, Q. D.; Jia, W. L.; Wang, S. *Inorg. Chem.* **2005**, *44*, 1332. (b) Jia, W. L.; McCormick, T.; Tao, Y.; Lu, J. P.; Wang, S. *Inorg. Chem.* **2005**, *44*, 5706.

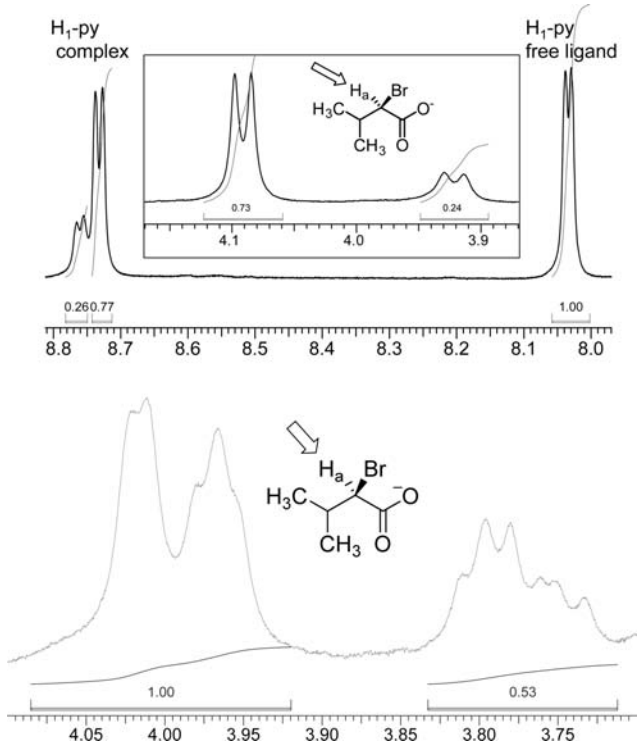

Figure 3. Top: Partial ^{1}H NMR spectrum of **1** with 0.5 equiv of Zn((*S*)-BrMeBu)$_2$ in CD_2Cl_2 at 298 K showing the H_1−py peaks and the H_a−BrMeBu peaks of the two diastereomers. Bottom: Partial ^{1}H NMR spectrum of **2**-Zn((*S*)-BrMeBu)$_2$ in CD_2Cl_2 at 203 K showing the H_a−BrMeBu peaks of diastereomers (the two sets of peaks at 4.00−3.93 and 3.83−3.72 ppm) and geometrical isomers (the multiple peaks within each set of diastereomer peaks).

tfa)$_2$ (see the Supporting Information), which complicates the diastereomer peak assignments in the H_1−py region. However, the two H_a−BrMeBu diastereomer peaks in the spectrum of **2**-Zn((*R*)-BrMeBu)$_2$ are well resolved at ∼223 K with a ∼2:1 ratio, similar to that of **1**-Zn((*R*)-BrMeBu)$_2$ (see Figure 3 and the Supporting Information). Hence, NMR experiments established that for both ligands **1** and **2** there is a preferential formation for one of the diastereomers with Zn((*R*)-BrMeBu)$_2$ [or Zn((*S*)-BrMeBu)$_2$].

Calculated Structures of 1-Zn(BrMeBu)$_2$. To determine which diastereomer of **1**-Zn(BrMeBu)$_2$ is favored, we performed DFT calculations using the *Gaussian 03* suite of programs at the B3LYP level with the 6-311G(d) basis set[9] for the diastereomers (*S*)-**1**-Zn((*R*)-BrMeBu)$_2$ and (*S*)-**1**-Zn((*S*)-BrMeBu)$_2$, assuming that a binding mode similar to that of Zn(tfa)$_2$ is adopted by the chiral zinc salt. Geometry optimization was performed for both diastereomers; the calculated structures for both diastereomers are shown in Figure 4. Indeed, the structures of the two diastereomers resemble that of **1**-Zn(tfa)$_2$. The computational results indicated an energy difference of ∼8.50 kJ/mol between (*S*)-**1**-Zn((*R*)-BrMeBu)$_2$ and (*S*)-**1**-Zn((*S*)-BrMeBu)$_2$, with the (*S*)-**1**-Zn((*S*)-BrMeBu)$_2$ complex [or (*R*)-**1**-Zn((*R*)-BrMeBu)$_2$] being the more stable diastereomer.

CD Spectral Response of Ligands 1 and 2 toward Zn((*R*)-BrMeBu)$_2$ and Zn((*S*)-BrMeBu)$_2$. To establish whether or not the racemic ligands **1** and **2** are capable of distinguishing chiral zinc(II) carboxylates, the CD spectral change of **1** and **2** toward Zn((*R*)-BrMeBu)$_2$ and Zn((*S*)-BrMeBu)$_2$ was examined. As shown in Figure 5 (and the titration diagram in the Supporting Information), the addition of either Zn((*S*)-BrMeBu)$_2$ or Zn((*R*)-BrMeBu)$_2$ to the solution of the racemate of **1** in CH_2Cl_2 (1.0×10^{-5} M) causes the appearance of a distinct CD spectrum in the 225−400 nm region, which increases in intensity with the amount of zinc(II) added. The CD spectrum of **1**-Zn((*S*)-BrMeBu)$_2$ is approximately the mirror image of that of **1**-Zn((*R*)-BrMeBu)$_2$ in the 250−400 nm region, supporting that the racemic **1** can indeed distinguish the enantiomers of Zn(BrMeBu)$_2$ by CD. Because Zn(BrMeBu)$_2$ has no absorption or a CD signal at $\lambda > 250$ nm, the intense CD bands in the 250−450 nm region are clearly a consequence of the electronic transitions of **1**, as supported by the UV−vis spectra of **1** and its zinc(II) complex (Figure 6). Significantly, at a fixed concentration of the ligand **1**, the intensity of the CD band at $\lambda_{max} = 320$ nm changes with the ee of the chiral zinc(II) carboxylate, as shown by Figure 5, an indication that the N,N-chelate **1** has the potential for quantitative determination of ee of Zn(BrMeBu)$_2$. The larger racemic chelate ligand **2** was found to display a similar CD spectral response upon addition of the chiral Zn(BrMeBu)$_2$ except that the CD band at 320 nm is much more intense and dominant, compared to that of **1** (Figure 6), consistent with the fact that the zinc(II) binding site in **2**-Zn(BrMeBu)$_2$ is similar to that of **1**-Zn(BrMeBu)$_2$ as established by the crystal structures **1**-Zn(tfa)$_2$ and **2**-Zn(tfa)$_2$ and ^{1}H NMR data. The relatively intense CD band at 320 nm in the spectrum of **2** with Zn(BrMeBu)$_2$ is consistent with the greater extinction coefficient of the corresponding absorption band, compared to that of **1**, as shown in Figure 6. Based on the NMR data and the calculated structures, the CD response of the racemic **1** and **2** toward the chiral Zn(BrMeBu)$_2$ shown in Figure 6 is likely a consequence of the CD spectral difference of the diastereomers and the preferential formation of one diastereomer.

Computational Study. To determine if the (*S*)-**1**-Zn((*R*)-BrMeBu)$_2$ and (*S*)-**1**-Zn((*S*)-BrMeBu)$_2$ [or (*R*)-**1**-Zn((*S*)-BrMeBu)$_2$ and (*R*)-**1**-Zn((*R*)-BrMeBu)$_2$] diastereomers have different CD spectra, TD-DFT calculations on this pair of diastereomers were performed using the optimized geometry parameters.[13] The first 25 singlet states were calculated and a $\sigma = 0.2$ eV line width was used.[14] The computed CD spectra of (*S*)-**1**-Zn((*R*)-BrMeBu)$_2$ and (*S*)-**1**-Zn((*S*)-BrMeBu)$_2$ are shown in Figure 7. These CD spectra are similar and match well with the experimental data in the 300−450 nm region, but a notable difference is evident in the short-wavelength region because of mostly the chiral carboxylate contributions (see the Supporting Information). Population analysis for the first 25 singlet excited states further confirms that most of the transitions with high oscillator strengths are

(13) (a) Crawford, T. D.; Tam, M. C.; Abrams, M. L. *J. Phys. Chem. A* **2007**, *111*, 12057. (b) Autschbach, J.; Jorge, F. E.; Ziegler, T. *Inorg. Chem.* **2003**, *42*, 2867.

(14) (a) Coughlin, F. J.; Oyler, K. D.; Pascal, R. A.; Bernhard, S. *Inorg. Chem.* **2008**, *47*, 974. (b) O'Boyle, N. M.; Tenderholt, A. L.; Langner, K. M. *J. Comput. Chem.* **2007**, *29*, 839.

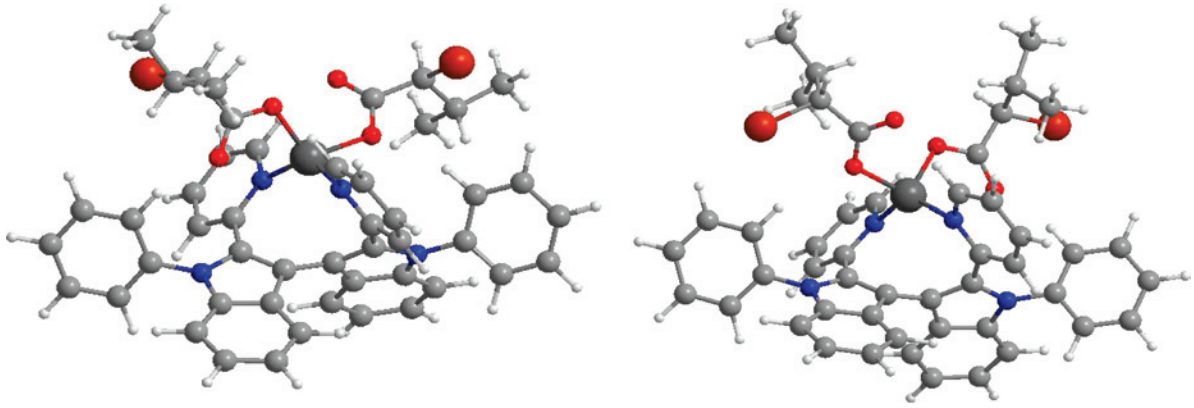

Figure 4. Calculated structures of (*S*)-**1**-Zn((*S*)-BrMeBu)$_2$ (left) and (*S*)-**1**-Zn((*R*)-BrMeBu)$_2$. Color code: C, gray; H, white; N, blue; O, red; Br, orange; Zn, dark gray.

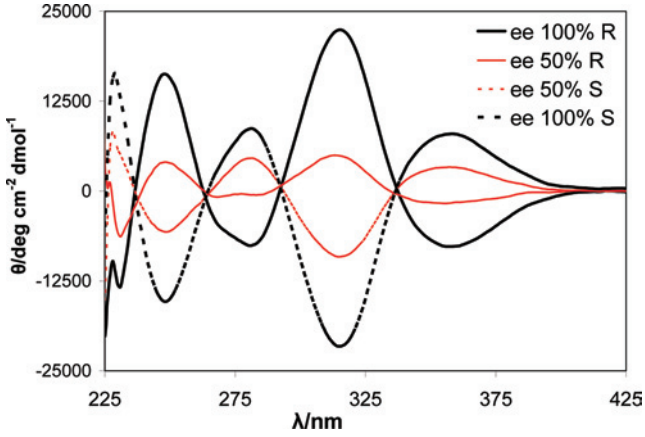

Figure 5. CD spectra of **1** (2.0×10^{-5} M) with 1 equiv of Zn(BrMeBu)$_2$ of varying ee in CH_2Cl_2.

dominated by 2-(2-py)indolyl parts of the ligand, which is consistent with the UV−vis data. The orbital diagrams for the highest occupied molecular orbital (HOMO), second HOMO, and three unoccupied orbitals for (*S*)-**1**-Zn((*S*)-BrMeBu)$_2$ shown in Figure 8 further illustrate that the low-energy electronic transitions in the complex involve the central part of ligand **1** with little contributions from zinc(II) or the carboxylate. The computational results also support that using the pure (*R*)-**1** or pure (*S*)-**1** alone will not be able to effectively distinguish the enantiomers of Zn(BrMeBu)$_2$ because of the similarity of the CD spectra of diastereomers (*S*)-**1**-Zn((*R*)-BrMeBu)$_2$ and (*S*)-**1**-Zn((*S*)-BrMeBu)$_2$ [or (*R*)-**1**-Zn(*R*-BrMeBu)$_2$ and (*R*)-**1**-Zn((*S*)-BrMeBu)$_2$]. On the basis of the computational results and NMR data, we can conclude that the distinct CD spectral response of racemic **1** toward Zn((*R*)-BrMeBu)$_2$ and Zn((*S*)-BrMeBu)$_2$ is due to the preferential formation of diastereometers (*R*)-**1**-Zn((*R*)-BrMeBu)$_2$ and (*S*)-**1**-Zn((*S*)-BrMeBu)$_2$, respectively, versus (*S*)-**1**-Zn((*R*)-BrMeBu)$_2$ and (*R*)-**1**-Zn((*S*)-BrMeBu)$_2$.

Selectivity and Fluorescent Response of 1 and 2 toward Zinc(II) Carboxylates. To find out if the atropisomeric N,N-chelate ligand **1** can discriminate other chiral zinc(II) carboxylates, we also examined the CD response of **1** toward Zn((*S*)-MeBu)$_2$, MeBu = 2-methylbutyrate.[10] Surprisingly, the addition of Zn((*S*)-MeBu)$_2$ to a solution of the racemic **1** under the same conditions as those used for Zn(BrMeBu)$_2$ did not yield any significant CD signal in the

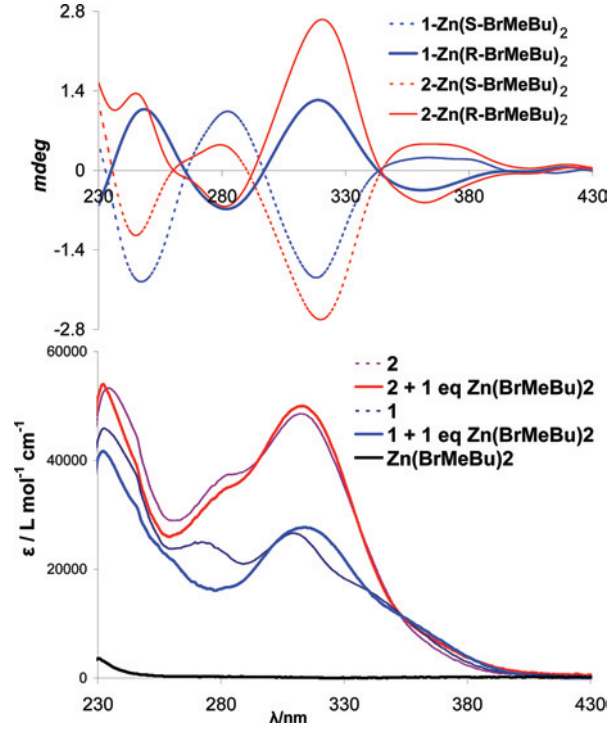

Figure 6. Top: CD spectra of **1** and **2** (1.0×10^{-5} M) with 1 equiv of chiral Zn(BrMeBu)$_2$ in CH_2Cl_2. Bottom: UV−vis spectra of **1**, **2**, and their complexes with Zn(BrMeBu)$_2$.

250−400 nm region. One possible explanation for the lack of CD response of **1** toward Zn((*S*)-MeBu)$_2$ is that 2-methylbutyrate is a stronger donor because of the electron-donating 2-methyl group, compared with 2-bromo-3-methylbutyrate, thus competing more effectively for the Zn^{II} ion and weakening the Zn^{II} binding with the chelate ligand **1**. Because **1** and **2** are highly fluorescent molecules, the relative binding strength of zinc(II) carboxylates can be compared qualitatively by fluorescent titration experiments. Indeed, we have observed that the addition of Zn(BrMeBu)$_2$ and Zn(tfa)$_2$ to a solution of the racemic **1** in CH_2Cl_2 causes a red shift of the emission band of **1**. Under the same conditions, Zn(OAc)$_2$ and Zn(MeBu)$_2$ have little impact on the emission spectrum of **1**, unless a large excess of the zinc(II) salt (>15 equiv) is added. For comparison, we also performed fluorescent titration with Zn(ClO$_4$)$_2$, where the ClO$_4^-$ anion is a well-known poor donor and the Zn^{II} ion is

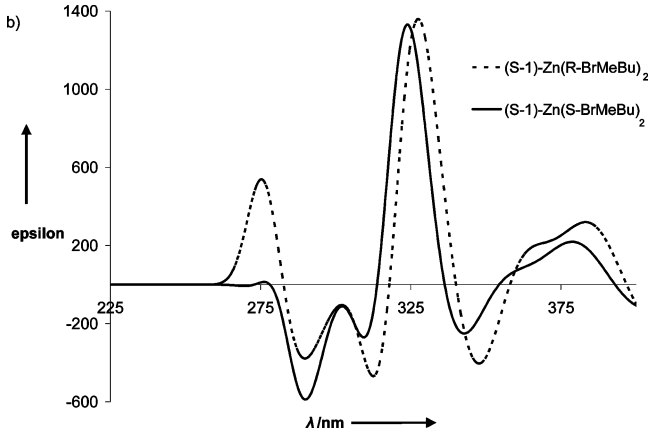

Figure 7. Computed CD spectra of (*S*)-**1**-Zn((*R*)-BrMeBu)$_2$ and (*S*)-**1**-Zn((*S*)-BrMeBu)$_2$.

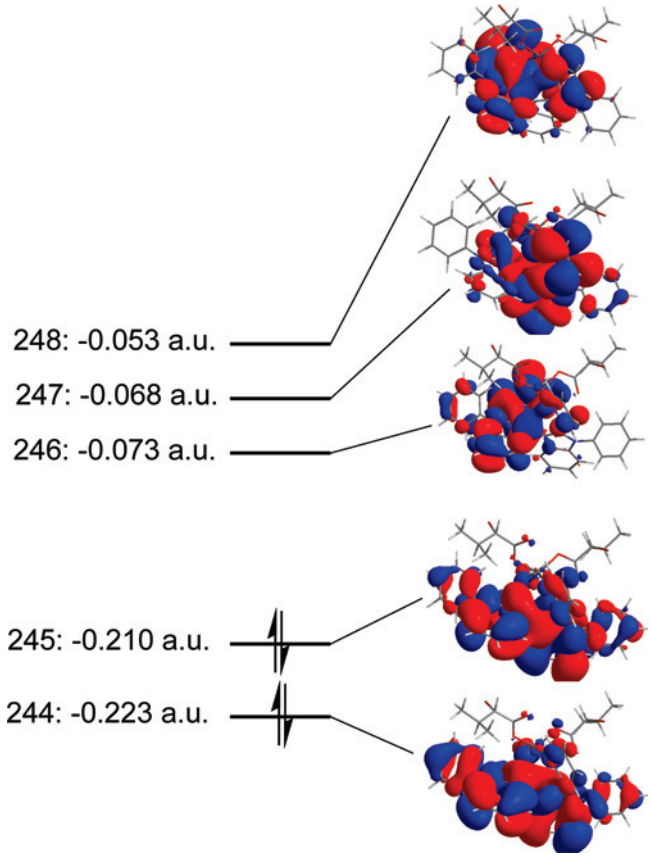

Figure 8. Diagram showing the frontier orbitals (orbital number and energy are shown on the left) of (*S*)-**1**-Zn((*S*)-BrMeBu)$_2$. The corresponding orbitals for (*S*)-**1**-Zn((*R*)-BrMeBu)$_2$ are similar with slight differences in the orbital energies.

expected to bind strongly with the chelate ligand. The addition of Zn(ClO$_4$)$_2$ to a solution of **1** causes a strong fluorescent quenching and an emission peak red shift as well. As shown in Figures 9 and 11, the fluorescent response of Zn(BrMeBu)$_2$ toward **1** and **2** is between those of Zn(tfa)$_2$ and Zn(ClO$_4$)$_2$. One notable difference between the chiral and nonchiral zinc(II) salts is the absence of isosbestic points in the chiral zinc(II) salt titration diagrams, which is consistent with the presence of diastereomers of the chiral zinc(II) complexes. From the Stern−Volmer plots shown in Figure 10, it is evident that the binding of Zn(BrMeBu)$_2$ to

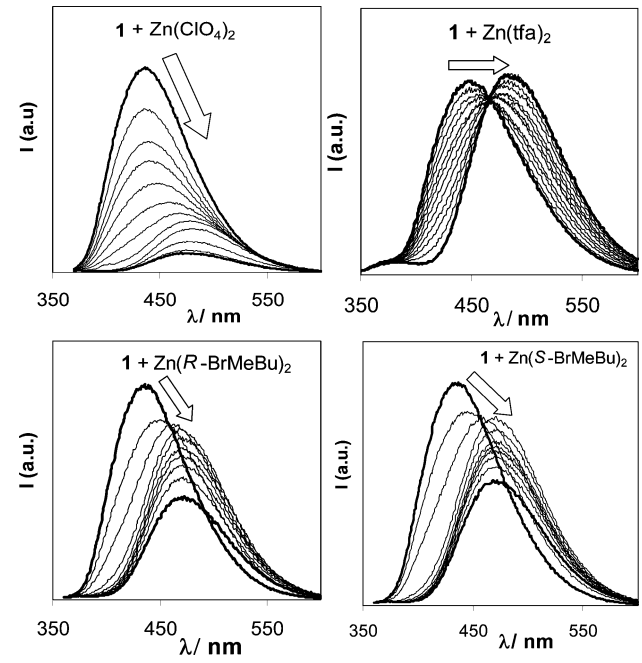

Figure 9. Fluorescent titration diagram of the solution of **1** (1.0×10^{-5} M) in CH_2Cl_2 with Zn(ClO$_4$)$_2$ (0.0−2.0 equiv), Zn(tfa)$_2$ (0.0−5.0 equiv), and Zn(BrMeBu)$_2$ (0.0−5.0 equiv), respectively.

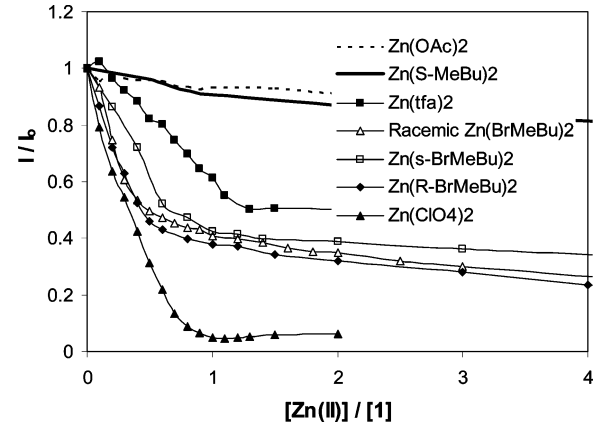

Figure 10. Stern−Volmer plots of the fluorescent titration of ligand **1** by zinc(II) salts.

ligand **1** is much stronger than that of Zn(tfa)$_2$, Zn(MeBu)$_2$, and Zn(OAc)$_2$ but much weaker than that of Zn(ClO$_4$)$_2$. Hence, the fluorescent data support that the lack of a CD response of ligand **1** toward the chiral Zn((*S*)-MeBu)$_2$ is due to the weak binding of this particular zinc(II) salt. The fluorescent response of ligand **2** toward zinc(II) carboxylates follows the same pattern as that of ligand **1**, as shown by data in Figure 11.

We also examined the CD response of **1** with the chiral (*S*)-2-bromo-3-methylbutyric acid [or (*R*)-2-bromo-3-methylbutyric acid] because the acid can interact with the atropisomeric ligand via hydrogen bonds. However, no significant CD spectral change was observed with the free acid. It is likely that the weak hydrogen bonds between the racemic host and the chiral guest are not sufficient to differentiate the diastereomers to produce significant CD signals. Therefore, the zinc(II) coordination to the atropisomeric ligand is clearly a key for distinguishing the two enantiomers of 2-bromo-3methylbutyrate via CD spectra. In

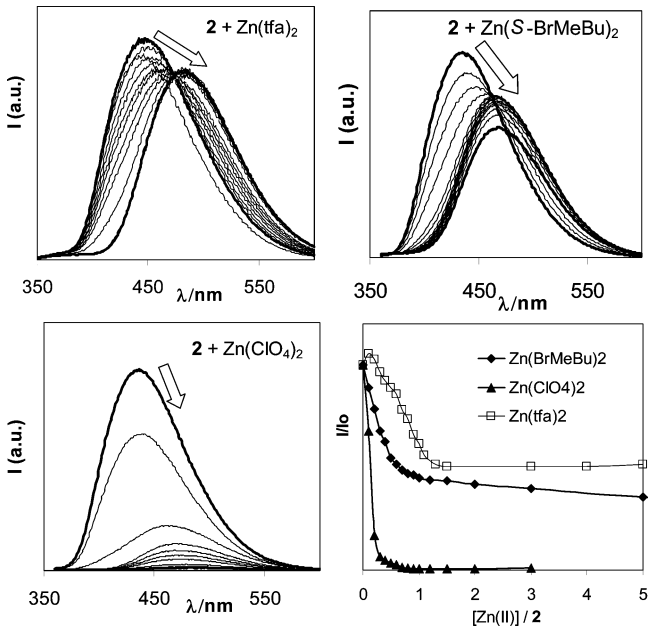

Figure 11. Fluorescent titration diagrams and Stern−Volmer plots of ligand **2** (1.0×10^{-5} M) in CH_2Cl_2 by three different zinc(II) salts.

other words, the Zn^{II} ion functions as a mediator to facilitate the recognition event between atropisomeric ligand and the chiral carboxylate.

In summary, two $Zn(tfa)_2$ complexes with two 2-(2-py)benzimidazolyl-based atropisomeric ligands, **1** and **2**, have been synthesized and structurally characterized. The Zn^{II} ion has been found to bind preferentially to the two central pyridyl rings in both ligands. We have demonstrated that the racemic ligands **1** and **2** are capable of distinguishing the enantiomers of $Zn(BrMeBu)_2$ and determining the ee by using CD spectroscopy. Furthermore, we have established that binding to the chelate site of ligands **1** and **2** by the chiral zinc(II) carboxylate is critical for achieving CD response. The binding strength of the carboxylate to the Zn^{II} ion was also found to play a key role in the CD response of **1** and **2** toward chiral zinc carboxylates, which may be used to discriminate different chiral carboxylates in conjunction with fluorescence spectra.

Acknowledgment. We thank the Natural Sciences and Engineering Research Council of Canada for financial support.

Supporting Information Available: Complete crystal data and fully labeled structural diagrams for **1**-$Zn(tfa)_2$ and **2**-$Zn(tfa)_2$, ^{1}H NMR titration data for **1** with $Zn(BrMeBu)_2$, variable-temperature ^{1}H NMR spectra for **1**-$Zn(tfa)_2$, **2**-$Zn(tfa)_2$, **1**-Zn((*S*)-$BrMeBu)_2$, and **2**-Zn((*S*)-$BrMeBu)_2$, fluorescent titration spectra of **1** with $Zn(OAc)_2$ and Zn((*S*)-$MeBu)_2$, and DFT and TD-DFT computational details. This material is available free of charge via the Internet at http://pubs.acs.org.

IC801269Z